Available online at www.sciencedirect.com
SCIENCE DIRECT®

Polymer 44 (2003) 6407–6417

polymer

www.elsevier.com/locate/polymer

Structural change in the Brill transition of Nylon *m/n* (2) conformational disordering as viewed from the temperature-dependent infrared spectral measurements

Yayoi Yoshioka[a,b], Kohji Tashiro[a,*], Chellaswami Ramesh[c]

[a]*Department of Macromolecular Science, Graduate School of Science, Osaka University, Toyonaka, Osaka 560-0043, Japan*
[b]*Technology Research Institute of Osaka Prefecture, Izumi, Osaka 594-1157, Japan*
[c]*Division of Polymer Chemistry, National Chemical Laboratory, Pune 411 008, India*

Received 20 March 2003; received in revised form 16 May 2003; accepted 16 June 2003

Abstract

The structural changes in the Brill transition of aliphatic Nylons *m/n* have been investigated by carrying out the temperature-dependent infrared spectral measurement for Nylon 6/10 $-[-NH-(CH_2)_6-NHCO-(CH_2)_8-CO-]_n-$, Nylon 6/12 $-[-NH-(CH_2)_6-NHCO-(CH_2)_{10}-CO-]_n-$ and Nylon 10/10 $-[-NH-(CH_2)_{10}-NHCO-(CH_2)_8-CO-]_n-$. They took the crystal structure of α-form at room temperature. By heating the samples up to the Brill transition temperature region, the conformation of the methylene segments was found to change remarkably from the all *trans*-zigzag form to the disordered conformation constructed by shorter *trans*-zigzag segments combined with some gauche bonds. At the same time, the twisting motion was found to occur around the CH_2–amide bonds. During this order-to-disorder transition of molecular conformation, the intermolecular hydrogen bonds were kept alive although they were weaker gradually with increasing temperature. The methylene segments sandwiched by NH groups $[NH(CH_2)_mNH]$ were found to be disordered more remarkably than those of $CO(CH_2)_nCO$ sequence due to the difference in torsional energy barriers around the CH_2-NH and CH_2-CO bonds.

Keywords: Nylon; Brill transition; Infrared spectra

---

1. Introduction

Aliphatic nylons show the so-called Brill transition in a high temperature region below the melting point [1]. The X-ray diffraction profile of typical α-crystal form changes to that of pseudohexagonal form above the transition temperature. But, in some cases, this profile change is not perfectly completed even when the sample is heated up to the melting point. Many papers were published so far to clarify the essential features of this Brill transition from the structural point of view [1–21], but still we have many unclear points about the concrete structural changes in the methylene sequences and the amide group parts as well as the hydrogen bond mode. For solving these problems, the vibrational spectroscopy may be one of the useful methods, which will give us concrete information about the chain conformational change. But, because of the complicatedness of the spectral profiles, the infrared and Raman spectra have not yet been interpreted enough clearly.

The infrared (and Raman) spectra of nylons are characterized by a series of progression bands as well as the bands coming from the amide groups. The progression bands are originated from the vibrational modes of the finite methylene sequences. Therefore the analysis of these progression bands may help us to clarify the structural change in the methylene segmental parts. For this purpose we have to assign these bands to the concrete vibrational modes. So far the several papers were reported to interpret the infrared spectra of some nylon samples, but the analysis was not necessarily consistent with each other [16,22–28]. In the previous paper, we proposed one new concept to solve the problem concerning the assignment of progression bands of nylons [29,30]. By utilizing this information the temperature dependence of progression bands was investigated for Nylon 10/10 and its model compounds, from which the conformational changes occurring in the Brill

---

[*] Corresponding author.

doi:10.1016/S0032-3861(03)00593-7

transitions could be revealed concretely [31,32]. The infrared bands characteristic of amide groups showed also the remarkable temperature dependence: the peak positions were shifted and the band intensities decreased remarkably with increasing temperature. From this observation, we could clarify the torsional motion of the amide groups in the Brill transition region. By combining the thus-obtained information on the amide groups with the conformational disordering in the methylene segments, the structural changes of molecular chains in the Brill transition were clarified in detail.

In the present paper, the concept developed in the vibrational analysis of Nylon 10/10 and its model compounds will be applied to the temperature-dependent infrared spectral data collected for Nylon 6/10 and Nylon 6/12 and the analyzed results will be compared with that of Nylon 10/10. These polymer samples have the different methylene sequential lengths, and therefore might be useful for the clarification of concrete role of the methylene segments in the Brill transition phenomenon of nylons.

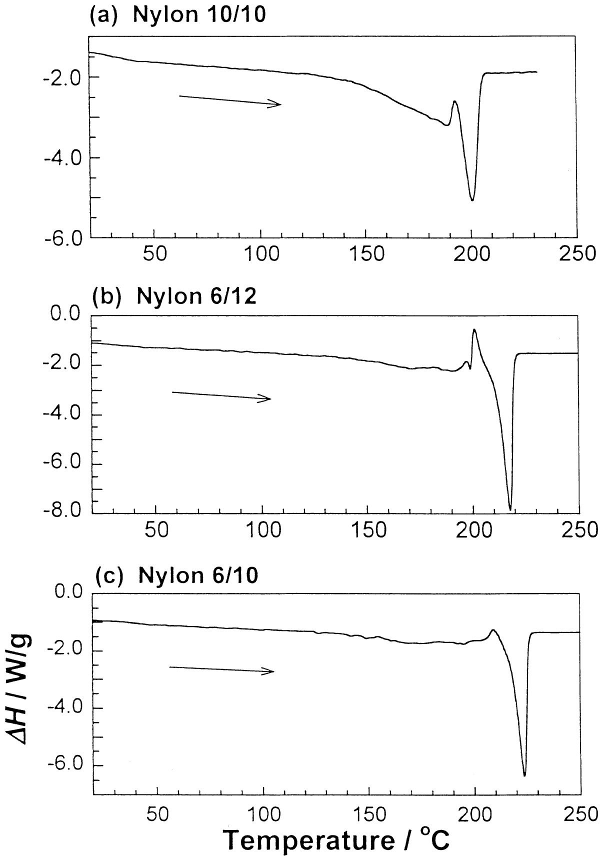

Fig. 1. DSC thermograms measured for (a) Nylon 10/10, (b) Nylon 6/12 and (c) Nylon 6/10 in the heating process.

2. Experimental

2.1. Samples

Nylon 6/10 and Nylon 6/12 were purchased from Aldrich chemicals. Nylon 10/10 was kindly supplied by the Shanghai Cellulose Works, Shanghai, China.

2.2. Measurements

The DSC thermograms were measured in the heating process by using a differential scanning calorimeter SEIKO DSC220CU under nitrogen gas atmosphere at the rate of 4 °C/min.

Thin films for the infrared spectral measurement were prepared by pressing the molten samples between a pair of KBr plates. Temperature dependence of infrared spectra was measured by using a Biorad FTS-60A/896 Fourier-transform infrared spectrometer at the resolving power of 2 cm^{-1}.

3. Results and discussion

3.1. DSC thermograms

Fig. 1(a)–(c) show the DSC thermograms measured for Nylon 10/10, Nylon 6/12 and Nylon 6/10, respectively, in the heating process from 20 °C to the melting region. In case of Nylon 6/10, a broad endothermic peak was detected in the region of 130–210 °C below the melting peak around 224 °C. The enthalpy changes ΔH for these two endothermic peaks were 39 and 52 J/g, respectively. In case of Nylon 6/12, a broad endothermic peak was observed in the region of 130–200 °C and the melting peak was at 218 °C. The ΔHs were 24 and 50 J/g, respectively. In the case of Nylon 10/10, a broad endothermic peak was detected in the region of 100–195 °C and a melting peak at 202 °C. The ΔHs were 46 and 29 J/g, respectively. Additionally a sharp exothermic peak was detected below the melting peak: 193 °C for Nylon 10/10, 201 °C for Nylon 6/12, and 209 °C for Nylon 6/10. It may correspond to the melt-recrystallization phenomenon or any phase transition before the melting. The latter possibility seems low as long as the infrared spectral data are analyzed as described in the present paper.

When the melting point is compared between Nylon 6/12 and 6/10, the former gives lower melting point because the $\mathrm{CO(CH_2)}_n\mathrm{CO}$ segment is longer ($n = 10 > 8$). On the other hand, the melting point of Nylon 10/10 is much lower than that of Nylon 6/10. The melting temperature gap between Nylon 6/10 and Nylon 10/10, 22 °C, is larger than that between Nylon 6/10 and Nylon 6/12, 6 °C. This difference is much larger than that expected from the difference in methylene sequence length between 6, 10 and 12. The $\mathrm{NH(CH_2)}_m\mathrm{NH}$ part is considered to have larger influence on the melting point because this part has higher mobility than that of $CO(CH_2)_nCO$ part, as will be discussed in a later section.

3.2. Temperature dependence of infrared spectra

3.2.1. Amide group bands

Temperature dependence of infrared spectra in the frequency region of 450–800 cm^{-1} is shown in Fig. 2(a)–(c) for Nylon 10/10, Nylon 6/12 and Nylon 6/10, respectively. The starting samples were obtained by slow cooling from the melt. At room temperature these polymers show the infrared bands typical of the planar–zigzag structure of the α-form as known from the characteristic bands at 580 cm^{-1} [amide VI (C=O out-of-plane mode)] and 690 cm^{-1} [amide V (NH out-of-plane mode)]. The infrared bands of the α-form were observed also at 3310 cm^{-1} [amide A (NH stretching mode)], 1635 cm^{-1} [amide I (C=O stretching mode)], 1535 cm^{-1} [amide II (C–N stretching mode)] and so on [26,33–41]. On heating up the samples, these amide bands were found to shift the positions. Fig. 3(a)–(c) show, respectively, the temperature dependence of the peak position estimated for the amide A, amide V and amide VI bands of Nylon 10/10, Nylon 6/12 and Nylon 6/10. The wavenumber of the amide A band is related directly with the strength of the intermolecular hydrogen bond. In the case of Nylon 6/12, for example, the band position shifted gradually to the higher frequency side with increasing temperature. Around 120–130 °C the slope of the temperature dependence is slightly changed, corresponding to the broad endothermic region in the DSC thermogram (Fig. 1(b)). The frequency shifted largely above 190 °C or in the melting region. These data indicated that the hydrogen bond became weaker gradually and this rate changed in the transition region. It became much weaker in the melting temperature region. The similar behavior of amide A band was observed for Nylon 6/10 and 10/10. Amide VI band shifted also to higher frequency side with increasing temperature for all the three cases, while Amide V band showed rather low-frequency shift or remained almost constant. These bands are considered to be affected also by the change in the hydrogen bonding strength. But, at the same time we need to consider that the Amide V and VI bands are sensitive to the twisting angles around the NH–CH_2 and CO–CH_2 bonds, respectively [26]. Broadening and slight peak position shift of these bands may correspond to an occurrence of twisting motion around the CH_2–amide bonds as well as the effect of hydrogen bonds. These various factors make the situation

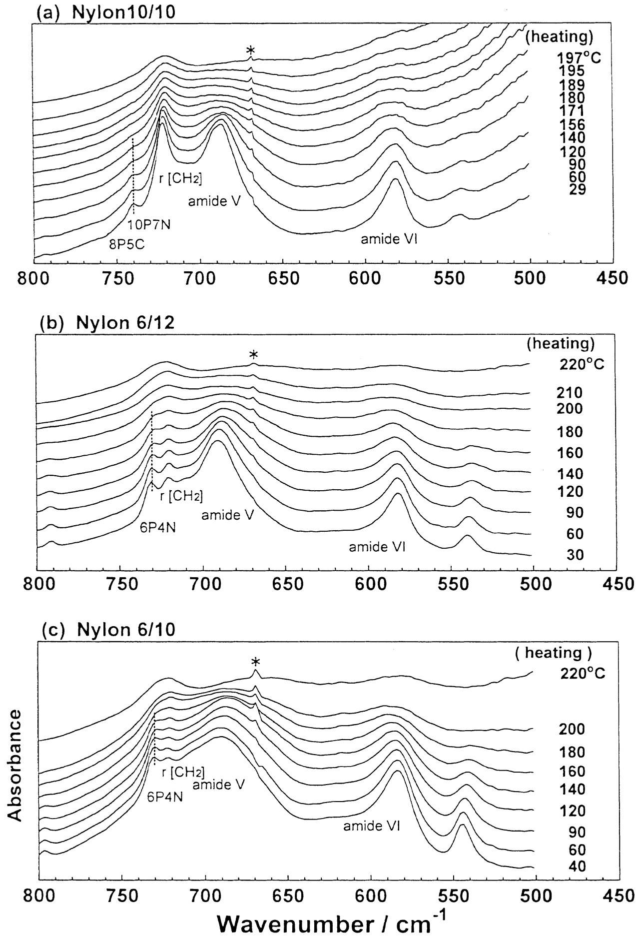

Fig. 2. Temperature dependence of infrared spectra measured for (a) Nylon 10/10, (b) Nylon 6/12 and (c) Nylon 6/10 in the heating process. Asterisks are the CO_2 gas bands.

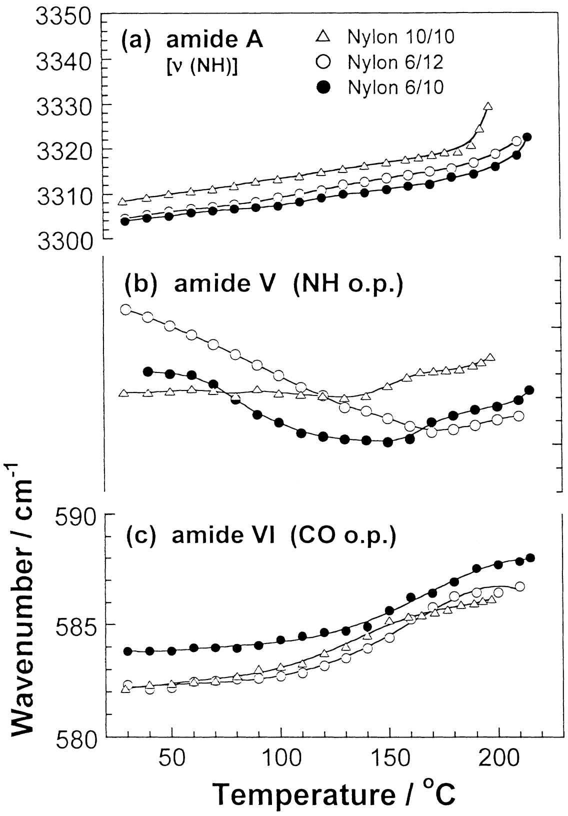

Fig. 3. Temperature dependence of vibrational frequency estimated for (a) amide A, (b) amide V and (c) amide VI bands of Nylon 10/10, 6/12, and 6/10 samples.

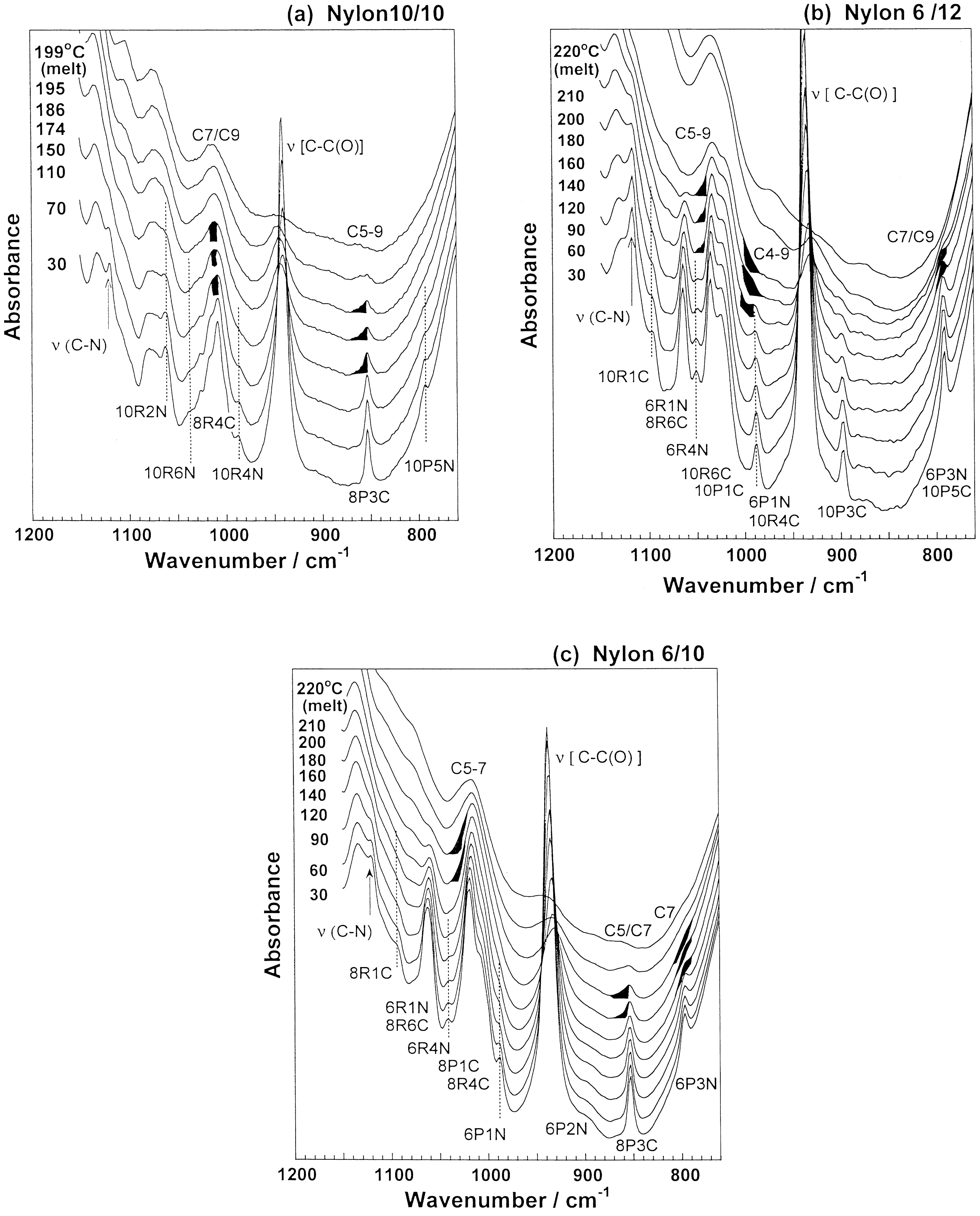

Fig. 4. Temperature dependence of infrared spectra measured for (a) Nylon 10/10, (b) Nylon 6/12 and (c) Nylon 6/10 in the heating process. The marks such as 8R4C are the progression bands of the methylene zigzag segments. C7, for example, indicates the band assigned to the progression band of n-C_7H_{16}. Shaded bands appeared in the high-temperature regions.

complicated and the temperature dependence of the Amide V and VI bands shown in Fig. 3 is difficult to interpret straightforwardly, different from the behavior of Amide A band. Similar but more remarkable change is detected for the bands of C–C(O) bond stretching mode (ν[C–C(O)]) around 937 cm^{-1} and C–N bond stretching mode [ν(C–N)] around 1120 cm^{-1} as shown in Fig. 4. These bands showed remarkable intensity decrement with increasing temperature. Besides, as shown in Fig. 5(a)–(c), the peak position and the band width were found to show large change. For example, in the case of Nylon 6/10, the peak position shift was accelerated in the transition region above 130 °C, and the band width also started to increase in this temperature region. The similar phenomenon was observed also for Nylon 6/12. In the case of Nylon 10/10 the essential behavior was the same but the change was more remarkable and the peak position of ν[C–C(O)] band shifted to higher frequency side. The similar higher frequency shift was observed for the model compounds of this polymer, $CH_3(CH_2)_9NHCO(CH_2)_8CONH–(CH_2)_9CH_3$ and $CH_3(CH_2)_8CONH(CH_2)_{10}NHCO(CH_2)_8CH_3$ [31,32]. It is difficult at present to know the reason for the different behavior of ν[C–C(O)] band between Nylons 6/12 and 6/10 and Nylon 10/10. On the other hand, for all these samples of polymers and model compounds commonly, the half-width of ν[C–C(O)] band increased gradually with increasing temperature and remarkably in the transition region. The band width is related generally with the activity of the thermal motion of the corresponding chemical group. The remarkable increase in half-width observed for ν[C–C(O)] band may reflect some enhancement of twisting motion around the CH_2–CO bond. The similar phenomenon is considered to occur also for the ν(C–N) band but was difficult to detect because of the influence of the neighboring intense bands (see Fig. 4). From all these results, we may say that the twisting of the amide–CH_2 bonds and the weakening of intermolecular hydrogen bond strength are accelerated in the broad endothermic peak region of DSC thermogram or in the Brill transition region.

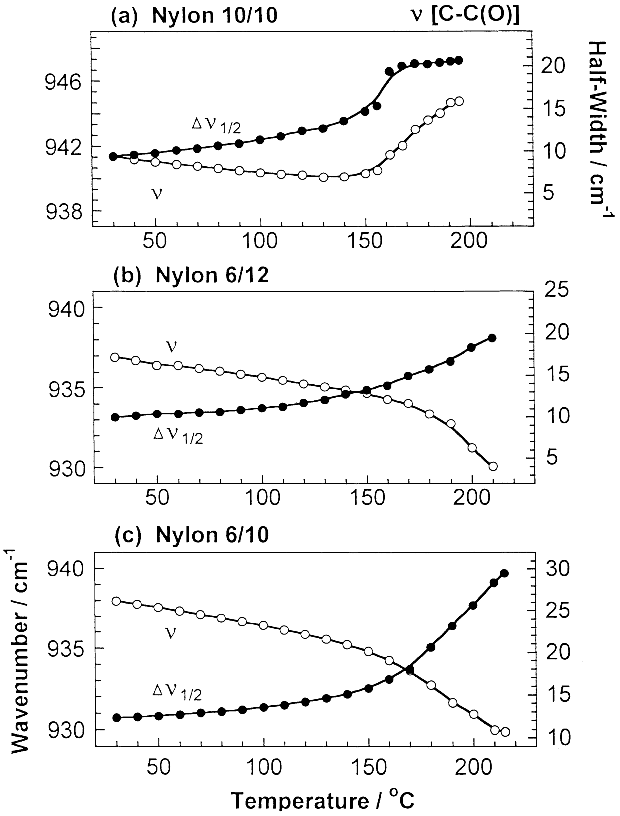

Fig. 5. Temperature dependence of vibrational frequency and half-width estimated for ν[C–C(O)] band of (a) Nylon 10/10, (b) Nylon 6/12 and (c) Nylon 6/10.

3.2.2. Methylene conformation

In Fig. 2(a)–(c), the band at 721 cm^{-1} is assigned to the most-in-phase methylene rocking mode [r(CH_2)] characteristic of the triclinic packing structure of *n*-alkane crystals. In cases of Nylon 6/12 and 6/10 the two bands at 721 and 731 cm^{-1} might be assumed as a pair due to the correlation splitting of the r(CH_2) mode in the orthorhombic packing cell of the methylene segments [42]. But the temperature dependence of the band intensity is different from that observed typically for *n*-alkane and orthorhombic polyethylene crystal. The band at 731 cm^{-1} is rather considered to correspond to one of the r(CH_2) progression bands, as will be discussed in a later section. When the sample was heated, the 721 cm^{-1} band decreased in intensity and was looked to approach the pattern intrinsic of the hexagonal packing structure of the methylene chains [43], but it was not clear because of broad spectral profile. On the other hand, the CH_2 scissoring band was observed in the 1465 cm^{-1} region at room temperature, the profile of which reflected the triclinic packing mode of methylene zigzag parts. With increasing temperature, the band intensity decreased and the profile became similar to that observed for the model compounds of Nylon 10/10 in the Brill transition region [31, 32], suggesting an existence of pseudohexagonal packing structure of conformationally disordered methylene segments [43–48]. But the definite conclusion was difficult to give because of broad spectral profile compared with the case of low-molecular-weight compounds.

This idea of conformational disordering in the methylene segments can be checked more explicitly when the infrared spectra in the frequency region of 760–1150 cm^{-1} are analyzed in detail. Fig. 4(a)–(c) show the temperature dependence of the infrared spectra in this frequency region. Many bands observed are due to the so-called progression bands of the methylene segments. For the analysis of progression bands a simply coupled oscillator model is used in general [49–53]. A local methylene vibrational mode is represented by an oscillator and these oscillators are coupled together with a phase angle ϕ. The ϕ is given by

$$\phi = k\pi/(m+1)$$

where m is an effective number of oscillators and $k = 1, 2, \ldots, m$. This simply coupled oscillator model was applied to the interpretation of the progression bands of nylons [22–27]. But, as reported in the previous papers [29,30], we had some inconsistency in the band assignments among a series of nylons and their model compounds. In order to solve this problem, we proposed one new concept. When we tried to assign the progression bands of nylons, we found that we needed to omit one methylene unit adjacent to the amide group, by which for the first time we could correspond the observed progression bands to the infrared bands of the n-alkanes with planar–zigzag conformation [29,30, 49–53]. Erase of one methylene unit adjacent to the amide group means a vibrational decoupling between the inner methylene segment and the outer methylene unit in the aliphatic nylon chain. For the planar–zigzag methylene chain of Nylon 6/10, for example, the methylene units included in the sequence NH–$(CH_2)_6$–NH are separated to a central $(CH_2)_4$ and 2 outer CH_2 parts. The vibrational bands coming from the $(CH_2)_4$ part can be assigned reasonably by referring to the bands observed for CH_3–$(CH_2)_4$–CH_3 (n-C_6H_{14}). Similarly, the $CO(CH_2)_8CO$ sequence is considered to give a series of progression bands coming from $(CH_2)_6$ segment, which is equivalent to CH_3–$(CH_2)_6$–CH_3 or n–C_8H_{18}. A methylene unit adjacent to the amide group gives a band at about 937 cm^{-1}?(ν[C–C(O)]), which is almost common to the various nylons and shows remarkable temperature dependence as discussed in the preceding section. In the same way, the methylene segments NH–$(CH_2)_6$–NH and CO–$(CH_2)_{10}$–CO of Nylon 6/12 are equivalent to those of CH_3–$(CH_2)_4$–CH_3 (n-C_6H_{14}) and CH_3–$(CH_2)_8$–CH_3 (n-$C_{10}H_{22}$), respectively. For Nylon 10/10 the methylene segments correspond to the CH_3–$(CH_2)_8$–CH_3 (n-$C_{10}H_{22}$) and CH_3–$(CH_2)_6$–CH_3 (n-C_8H_{18}) from the vibrational spectroscopic point of view. The progression bands assigned to the modes of equivalent n-alkanes are indicated by small symbols in Fig. 4. For example, 8P3C means that this band is equivalent to the progression band of CH_2 rocking (P) mode of n-C_8H_{18} with a phase angle between the neighboring methylene groups $\phi = k\pi/(m+1) = 3\pi/(6+1) = 3\pi/7$ [a total number of effec-

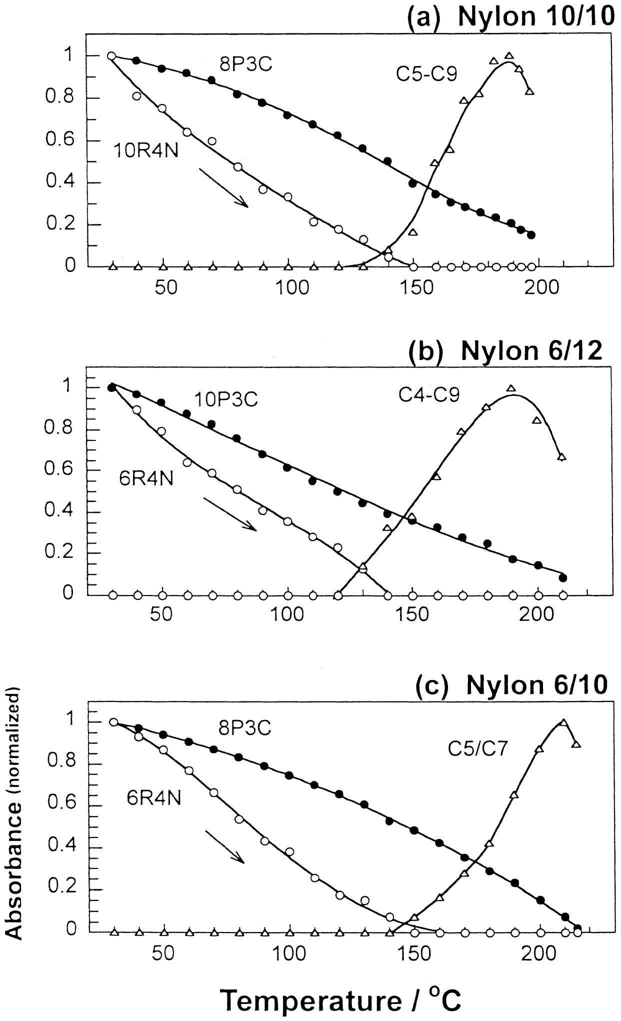

Fig. 6. Temperature dependence of normalized absorbance estimated for various methylene progression bands of (a) Nylon 10/10, (b) Nylon 6/12 and (c) Nylon 6/10. The meaning of the marks such as 8P3C is referred to in the text. The absorbance of newly appeared progression band (C7/C9 and so on) was estimated for the bands at 858 cm^{-1} for Nylon 10/10 and 6/10 and at 1000 cm^{-1} for Nylon 6/12.

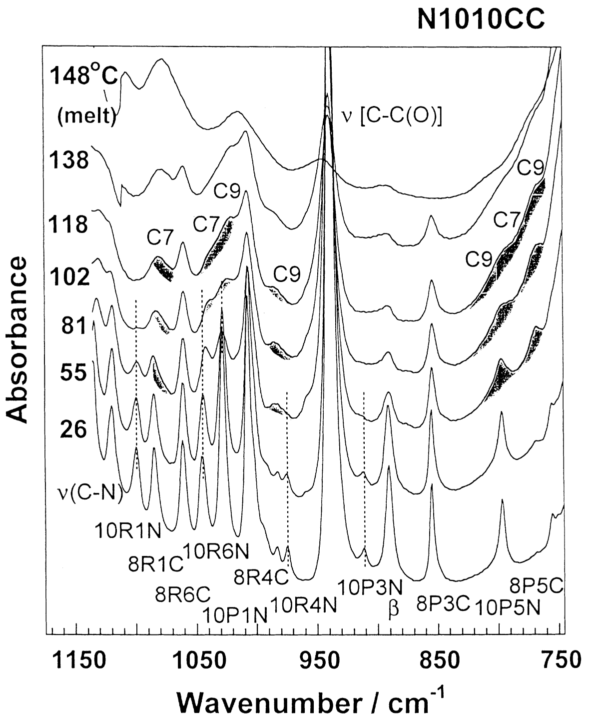

Fig. 7. Temperature dependence of infrared spectra measured for the model compound of Nylon 10/10, $CH_3(CH_2)_9NHCO(CH_2)_8CONH$–$(CH_2)_9CH_3$, in the frequency region of 750–1150 cm^{-1}. The meaning of the marks such as 10P3N, etc. is referred to in the text. The shaded bands with the marks C7 and C9 are the progression bands assigned to the equivalent n-C_7H_{16} and n-C_9H_{20}, respectively. The original progression bands decreased in intensity and the new progression bands (shaded bands) appeared in stead.

tive oscillators $m = 6$ and the coefficient $k = 3$]. A methylene chain consisting of 6 methylene units is equivalent to n-C_8H_{18} when two methyl groups are added as end groups. The 'C' indicates the methylene sequence of the carbonyl group side [$CO-(CH_2)_m-CO$]. In the spectra shown in Fig. 4, we can classify the bands into two species: the methylene sequence of NH side (N) and the methylene sequence of CO side (C).

When the temperature was raised, some of the progression bands were found to decrease in intensity remarkably. Some bands disappeared perfectly and new bands appeared in high temperature region as shown in Fig. 4. For example, in the case of Nylon 6/10, the bands 6P1N (988 cm^{-1}), 6R4N (1040 cm^{-1}), 8R1C (1100 cm^{-1}), 6T2N (1274 cm^{-1}), 8W4C (1331 cm^{-1}), etc. disappeared perfectly in the transition region, where R, W and T indicate the CC stretching mode, the CH_2 wagging mode and the CH_2 twisting mode, respectively. Fig. 6(c) shows the relative intensity of some typical progression bands of Nylon 6/10 plotted against temperature. As the temperature increased, the progression bands coming from the methylene segments of the NH side decreased in intensity more remarkably than those of the CO side, indicating higher chain flexibility or easiness of conformational disordering in the methylene segments of $NH(CH_2)_mNH$ than the $CO(CH_2)_nCO$ part. These observations were made for all the nylons discussed here.

When the progression bands of the methylene units disappeared in the transition temperature region, new bands were detected although they were broad and weak in general. This phenomenon was observed clearly for the model compounds of Nylon 10/10 as reproduced in Fig. 7 [31,32]. The bands at 981, 1022, 1038 and 1077 cm^{-1}, etc. correspond to these newly appeared ones. But such an observation was a little difficult for the polymers. In the case of Nylon 6/10, for example, the new bands were detected at 790, 860, 1028, 1200 and 1245 cm^{-1}, etc. (see Fig. 4(c)). In Fig. 6, the absorbance of a newly appeared band is plotted against temperature. They are considered to correspond to the progression bands of n-C_7H_{16} and n-C_5H_{12}, indicating that the fully extended *trans*-zigzag methylene sequence changes to the shorter zigzag segment of $(CH_2)_5-(CH_2)_3$ by an invasion of some gauche bonds. This conformational disordering is considered to occur more remarkably in the methylene segments of NH side than those of CO side, as speculated from the results shown in Figs. 6 and 7. The similar observations were made for Nylon 6/12 and Nylon 10/10. In the case of Nylon 6/12, the newly appeared bands were assigned to the progression bands of n-C_9H_{20}–n-C_4H_{12}. In the case of Nylon 10/10, they were assigned to those of n-C_9H_{20}–n-C_5H_{12}.

Another important observation is that the decreasing rate of the progression band intensity is almost the same when the progression band of the same methylene sequential

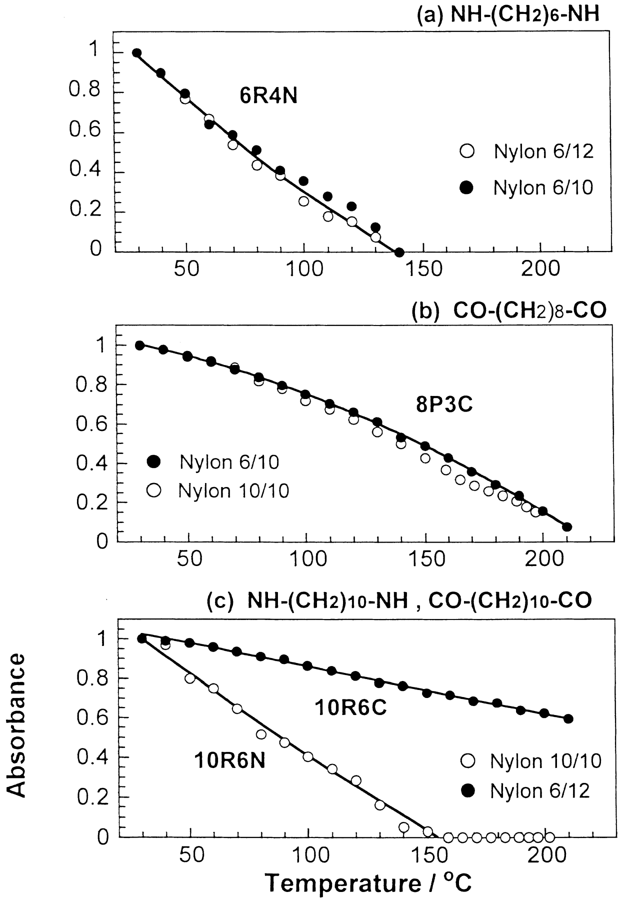

Fig. 8. Temperature dependence of normalized absorbance estimated for the progression band of the same methylene sequence compared between Nylons 10/10, 6/12 and 6/10. The meaning of the marks such as 8P3C is referred to in the text.

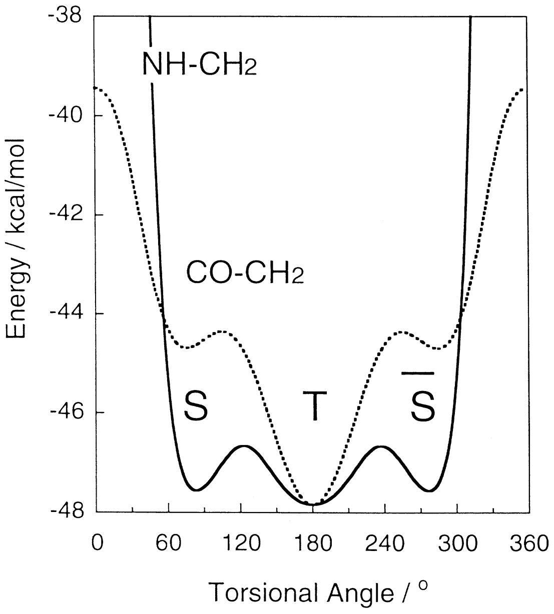

Fig. 9. Potential energy curves of a nylon segment $CH_3CH_2CH_2-NHCO-CH_2CH_2CH_3$ calculated as functions of torsional angle around the CH_2-NH (solid line) and CH_2-CO bonds (broken line). The calculation was made with Cerius^2 (Accelrys Inc.) on the basis of COMPASS force field [Sun H. J Phys Chem 1998;B102:7338].

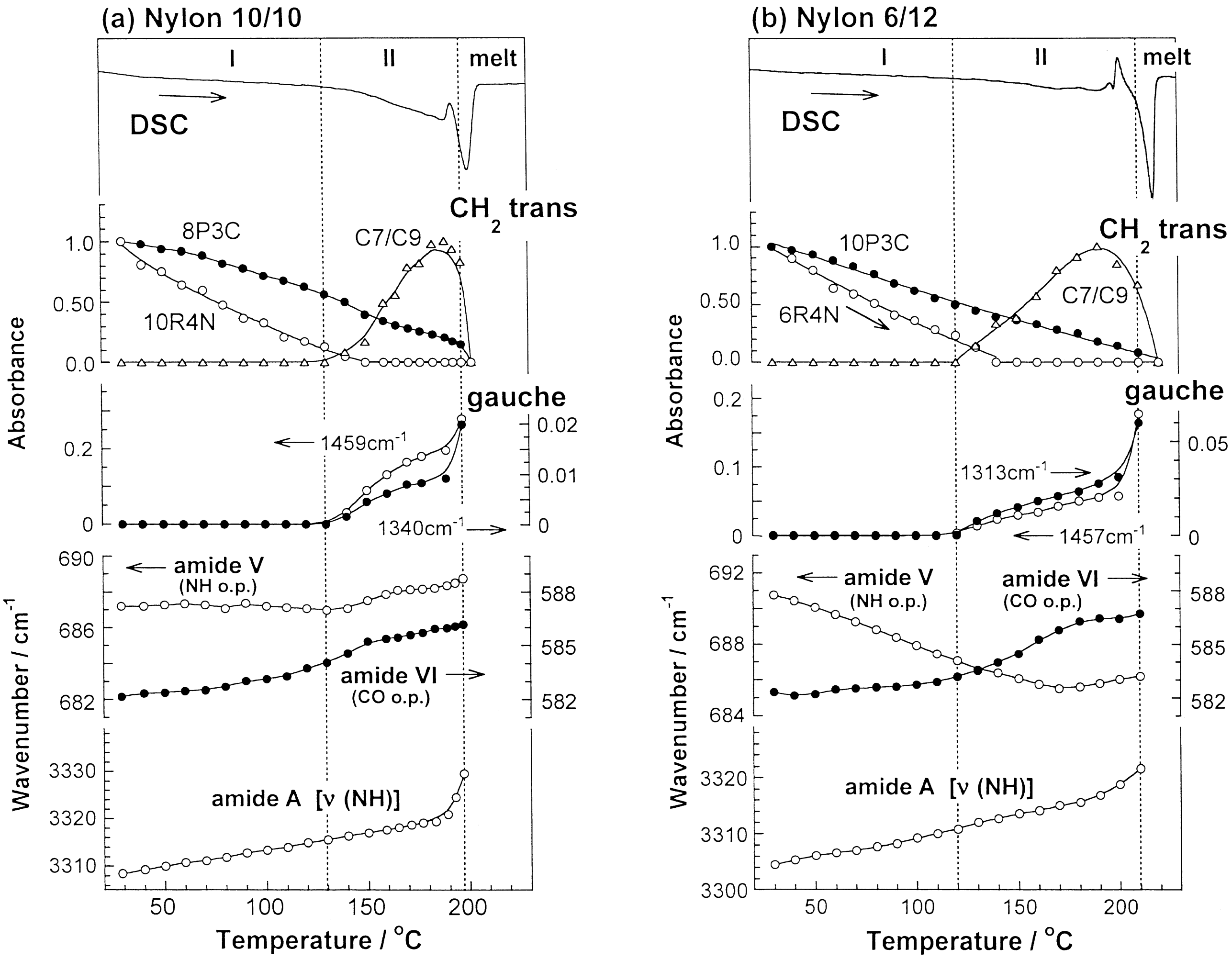

Fig. 10. Temperature dependence of infrared data evaluated for (a) Nylon 10/10, (b) Nylon 6/12 and (c) Nylon 6/10 in comparison with the DSC thermograms (heating process).

length is compared, as shown in Fig. 8(a) and (b). In these nylons, we have three kinds of methylene segments: $(CH_2)_6$, $(CH_2)_8$ and $(CH_2)_{10}$. As seen in Fig. 8(a), the progression band intensity of the $NH(CH_2)_6NH$ part (6R4N) showed essentially the same intensity change between Nylon 6/12 and Nylon 6/10. Similar observation was made for the bands of $CO(CH_2)_8CO$ (8P3C) of Nylon 6/10 and Nylon 10/10 as shown in Fig. 8(b). The remarkable difference in the intensity reduction rate was observed between the methylene progression bands of the NH and CO sides even when the methylene segmental length was apparently the same (see Fig. 8(c)). Therefore the effective methylene segments are considered to show essentially the same temperature dependence as long as the number of methylene units is the same and these methylene units are sandwiched in between the same side of amide group, i.e. the NH side (or the CO side). It is emphasized here again that the methylene progression bands of the NH side show more remarkable intensity decrement than those of the CO side. This can be observed in Figs. 6 and 8. The solid-state NMR reported the higher mobility of $NH(CH_2)_mNH$ segment than $CO(CH_2)_nCO$ segment in Nylon 6/6 [7,8]. The present infrared data are consistent with it. When the conformational energy is calculated as a function of torsional angle around the CH_2–amide bond, it is found that the energy barrier of the torsion around the CH_2–amide bond is lower for $NH–CH_2$ bond than for $CH_2–CO$ bond (see Fig. 9). This seems to be related with the above-mentioned difference in thermal behavior of the methylene progression bands. As pointed out already, the inner methylene segments are vibrationally decoupled with the terminal methylene unit adjacent to the amide group. If the inner methylene units and terminal methylene units are chemically separated, the thermal behavior of the inner methylene segment should be the same between the NH and CO sides. But, actually the methylene units are connected by strong covalent bonds. Therefore, even when the coupling is lost about the local vibrational modes at higher frequencies, the twisting motion around the CH_2–amide bond is considered to relate strongly with the segmental motion of the whole methylene sequence. Higher

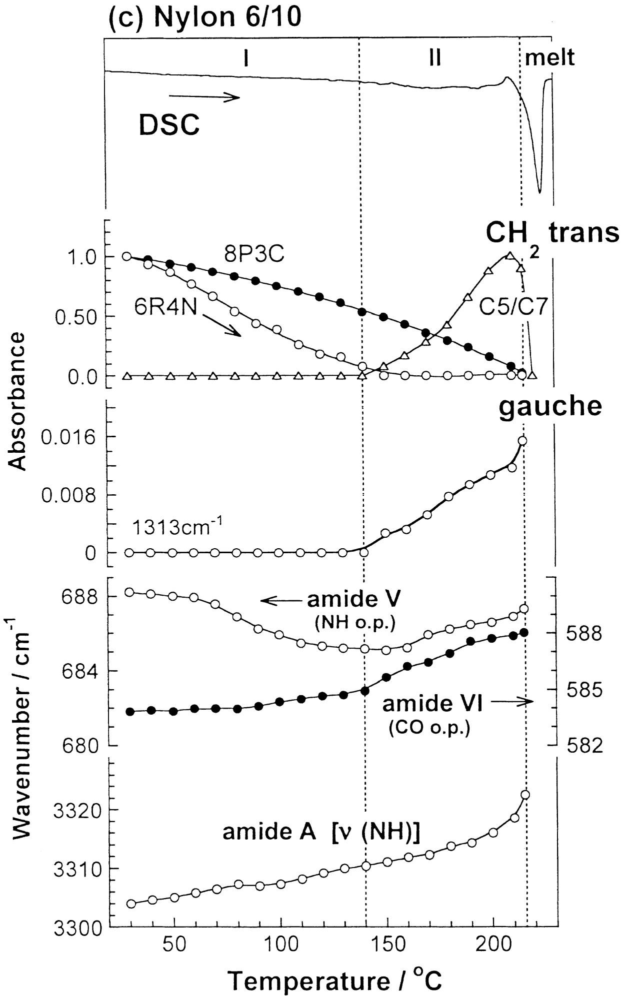

Fig. 10 (*continued*)

activity of torsional motion around the CH_2–NH bond may cause easier thermal motion of the methylene segments of NH side. The torsional motion around the CH_2–CO bond may be difficult to occur because of higher torsional barrier, resulting in lower mobility of the methylene units of the CO side. The difference in temperature dependence of the methylene progression bands between the NH and CO sides, shown in Figs. 6 and 8, may come from such a situation.

3.3. Structural disordering of Nylon m/n

As discussed above, the infrared spectral changes were analyzed about the three different kinds of vibrational groups. Fig. 10 shows the temperature dependence of the infrared data evaluated for these different groups in comparison with the DSC thermograms. In the temperature region I below the Brill transition region, the slight changes were observed for amide V, VI and amide A bands. The methylene progression bands in the NH side already decreased in intensity with increasing temperature. In the region II or the Brill transition region, the intensity of the NH side progression bands became zero and that of the CO-side bands decreased gradually. At the same time the progression bands of shorter zigzag chain segments appeared. The gauche band intensity (at 1340 and 1459 cm^{-1}) increased in parallel. The amide V and VI bands shifted and the amide A band frequency changed at the same time. In the temperature region III the sample was melted. The structural changes extracted from these observations may be summarized as follows. (i) The CH_2–NH and CH_2–CO bonds are twisted more or less in the transition temperature region, as seen from the large frequency shift of the amide V and VI bands as well as the remarkable change of vibrational frequency, intensity and half-width of the C–C(O) and C–N stretching bands. (ii) At room temperature, the methylene segments are packed in a triclinic subcell structure similar to that of *n*-alkanes [54] and this packing mode changes gradually to the hexagonal type, although the spectral change is broad and difficult to detect explicitly compared with the case of low-molecular-weight model compounds. (iii) The methylene segments take the planar–zigzag conformation at room temperature

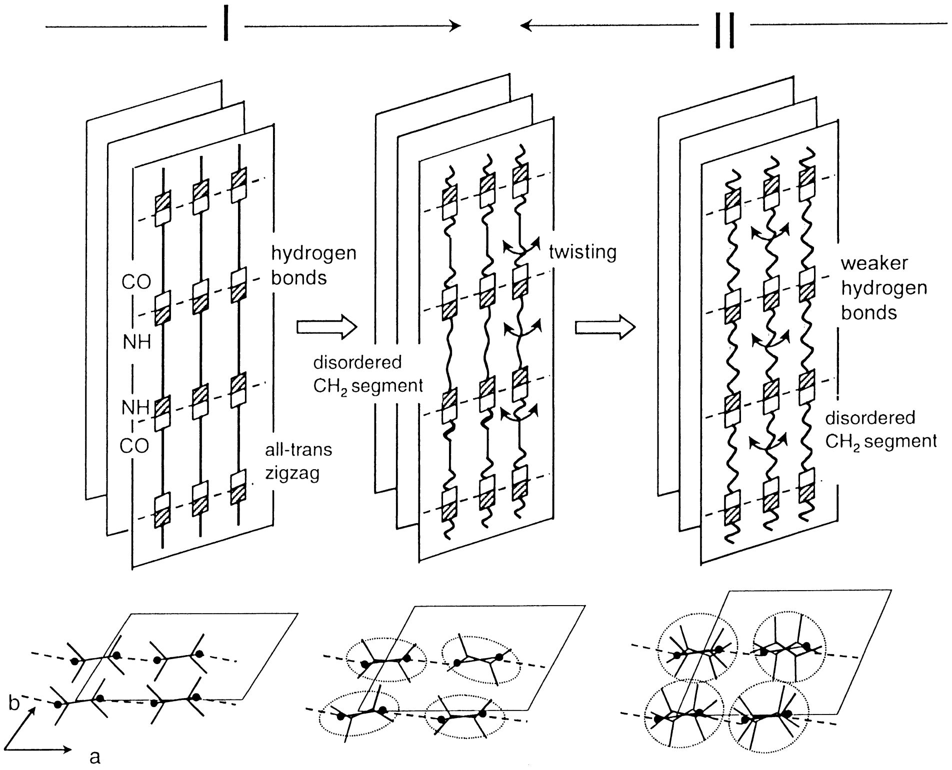

Fig. 11. An illustration of structural change in the Brill transition of Nylon *m*/*n*. The temperature regions I and II correspond to those shown in Fig. 10. The thick solid lines indicate the methylene segments of all-*trans* zigzag conformation. The pictures shown in the lower side are the subcell structures of the methylene chain segmental parts viewed along the chain axis.

and the corresponding progression bands are assigned reasonably. As seen in Fig. 10 the intensity of the progression bands decreased largely with increasing temperature. This intensity decrement is more remarkable for the methylene segments of the N–H side and some conformational disordering occurs already in the temperature region I. In the region II the progression bands of the CO side decreased in intensity also and the bands of shorter methylene segments increased in intensity. The gauche bands were also observed in parallel. In this way the methylene segments are conformationally disordered in the Brill transition region II. (iv) The intermolecular hydrogen bond strength is reduced at higher temperature as known from the high frequency-shift of the amide A band, but the hydrogen bond is kept even in the transition region. In the melting region the bond strength becomes much weaker and the number of hydrogen-bond-free amide groups is increased as seen from the intensity increment of the corresponding infrared bands (3345 cm^{-1}) [38].

The structural change occurring in the Brill transition region of Nylon *m*/*n* is shown in Fig. 11. At room temperature, the crystal structure is of the α-form. The all-*trans* zigzag chains are packed to form a sheet structure through the intermolecular hydrogen bonds. These sheets are stacked together by weak van der Waals interactions. When the temperature increases, the methylene segmental parts start to disorder and the amide–CH$_2$ bonds change the twisting angles. The methylene segments of the NH side are more highly disordered than those of the CO side. As discussed in the previous section, the twisting motion around the CH$_2$–amide bond is considered to relate with the segmental motion of the methylene units. Higher twisting motion of the CH$_2$–NH bond seems to result in the easier conformational disordering of the NH-side methylene segments. In parallel to these structural changes, the hydrogen bonds become weaker gradually. In the Brill transition region (region II in Fig. 10), these changes become remarkable. The methylene segments are conformationally disordered with an invasion of gauche bonds and the effective lengths of *trans*-zigzag methylene parts become shorter. The triclinic packing structure is kept in average, but it approaches gradually to the pseudo-hexagonal packing mode as seen from the X-ray diffraction data [1–6,9–15,17–21].

4. Conclusions

In the present paper, the structural change in the Brill transition was investigated for Nylons 10/10, 6/12 and 6/10 by measuring the temperature dependence of infrared spectra as well as the DSC thermograms. For all these samples, the common structural features in the Brill transition were extracted. The structural change is of the order-to-disorder type. The conformation of all-*trans* zigzag methylene segments is shortened by an invasion of gauche bonds. This tendency is more remarkable for the $NH(CH_2)_mNH$ part than the $CO(CH_2)_nCO$ part. Such a conformational disordering in the methylene segment is related strongly with the twisting motions about the amide–CH_2 bonds. The intermolecular hydrogen bonds are kept but become weaker.

So far the change of X-ray diffraction pattern from triclinic to pseudo-hexagonal type was considered to be useful for tracing the Brill transition phenomenon. It was said that there occurred no Brill transition if the X-ray diffraction did not change completely from the triclinic to pseudohexagonal pattern. But the structural change is not a real transformation of the triclinic packing to the pseudo-hexagonal mode. The intermolecular hydrogen bonds are kept in the transition region, making the real hexagonal packing of the rotating chains impossible. Therefore the X-ray diffraction profile change is not needed to complete in the Brill transition [2]. More important and essential structural feature is a conformational disordering in both the methylene and CH_2–amide parts of the molecular chains. They spontaneously result in the change of the X-ray diffraction pattern. The conformational disordering occurs in a wide temperature region. This is not because of the broad molecular weight distribution and many structural defects. In fact, the broad transition behavior was detected even for the low-molecular-weight model compounds with explicitly defined chemical formulae. Therefore the Brill transition of nylons may be assumed as a structural disordering process which occurs in an appreciably wide temperature region.

References

[1] Brill R. J Prakt Chem 1942;161:49.
[2] Itoh T. Jpn J Appl Phys 1976;15:2295.
[3] Newman BA, Sham TP, Pae KD. J Appl Phys 1976;48:4092.
[4] Starkweather HW, Jones GA. J Polym Sci, Polym Phys Ed 1981;19:467.
[5] Kim KG, Newman BA, Scheinbeim JI. J Polym Sci, Polym Phys Ed 1985;23:2477.
[6] Biangardi HJ. J Macromol Sci, Phys B 1990;29:139.
[7] Hirschinger J, Miura H, Gardner KH, English AD. Macromolecules 1990;23:2153.
[8] Wendoloski JJ, Gardner KH, Hirschinger J, Miura H, English AD. Science 1990;247:431.
[9] Murthy NS, Curran SA, Aharoni SM, Minor H. Macromolecules 1991;24:3215.
[10] Radusch HJ, Stolp M, Androsch R. Polymer 1994;35:3568.
[11] Hill MJ, Atkins DT. Macromolecules 1995;28:2642.
[12] Jones NA, Atkins EDT, Hill MJ, Cooper SJ, Franco L. Polymer 1997;38:2689.
[13] Jones NA, Cooper SJ, Atkins EDT, Hill MJ, Franco L. J Polym Sci, B (Polym Phys Ed) 1997;35:675.
[14] Cooper SJ, Atkins EDT, Hill MJ. Macromolecules 1998;31:8947.
[15] Franco L, Cooper SJ, Atkins EDT, Hill MJ, Jones NA. J Polym Sci, B (Polym Phys Ed) 1998;36:1153.
[16] Vasanthan N, Murthy NS, Bray RG. Macromolecules 1998;31:8433.
[17] Murthy NS, Wang Z, Hisao BS. Macromolecules 1999;32:5594.
[18] Ramesh C, Gowd EB. Macromolecules 1999;32:3721.
[19] Jones NA, Atkins EDT, Hill MJ. J Polym Sci, B (Polym Phys) 2000;38:1209.
[20] Ramesh C, Gowd EB. Macromolecules 2001;34:3308.
[21] Yang X, Tan S, Li G, Zhou E. Macromolecules 2001;34:5936.
[22] Schneider B, Schmidt P, Wichterle O. Coll Czech Chem Commun 1962;27:1749.
[23] Jakes J, Schmidt P, Schneider B. Coll Czech Chem Commun 1965;30:996.
[24] Jakes J. J Polym Sci, C 1967;16:305.
[25] Jakes J, Krimm S. Spectrochimica Acta 1971;27A:19.
[26] Jakes J, Krimm S. Spectrochimica Acta 1971;27A:35.
[27] Raman R, Deopura LB, Varma DS. Indian J Text Res 1977;2:56.
[28] Cooper SJ, Coogan M, Everall N, Priestnall I. Polymer 2001;42:10119.
[29] Yoshioka Y, Tashiro K. Polym Prepr Jpn 2002;51:2056.
[30] Yoshioka Y, Tashiro KJ. Polym Sci B (Polym Phys) 2003;41:1294.
[31] Tashiro K, Yoshioka Y, Hama H, Yoshioka A. Macromolecular Symposia 2003; in press.
[32] Yoshioka Y, Tashiro K. Polym Prepr Jpn 2002;51:2057.
[33] Bunn CW, Garnar EV. Proc Roy Soc 1947;A189:39.
[34] Miyake A. J Polym Sci 1960;44:223.
[35] Arimoto H. J Polym Sci, A 1964;2:2283.
[36] Matsubara I, Itoh Y, Shinomiya M. Polym Lett 1966;4:47.
[37] Komatsu T, Makino D, Kobayashi M, Tadokoro H. Rep Prog Polym Phys Jpn 1970;13:1051.
[38] Skrovanek DJ, Painter PC, Colemen MM. Macromolecules 1986;19:699.
[39] Maddam WF, Royaud IAM. Spectrochimica Acta 1991;47A:1327.
[40] Schmidt P, Hendra PJ. Spectrochimica Acta 1994;50A:1999.
[41] Yu HH. Mater Chem Phys 1998;56:289.
[42] Snyder RG. J Chem Phys 1979;71:3229.
[43] Tashiro K, Sasaki S, Kobayashi M. Macromolecules 1996;29:7460.
[44] Snyder RG, Maroncelli M, Qi SP, Strauss HL. Science 1981;214:188.
[45] Maroncelli M, Qi SP, Strauss HL, Snyder RG. J Am Chem Soc 1982;104:6237.
[46] Maroncelli M, Strauss HL, Snyder RG. J Chem Phys 1985;82:2811.
[47] Hagemann H, Strauss HL, Snyder RG. Macromolecules 1987;20:2810.
[48] Kim Y, Strauss HL, Snyder RG. J Phys Chem 1989;93:7520.
[49] Snyder RG. J Mol Spectrosc 1960;4:411.
[50] Nielsen JR, Holland RF. J Mol Spectrosc 1960;4:448.
[51] Nielsen JR, Holland RF. J Mol Spectrosc 1961;6:394.
[52] Snyder RG, Schachtschneider JH. Spctrochimica Acta 1963;19:85.
[53] Schachtschneider JH, Snyder RG. Spctrochimica Acta 1963;19:117.
[54] Sirota EB, King HE, Singer Jr DM, Shao HH. J Chem Phys 1995;98:5809.